EFFECT OF SURFACE SPIRAL PROTUBERANCES ON THE DRAG CRISIS IN A CIRCULAR CYLINDER

Kyoto University Student Member ○Omar Marey
Kyoto University Regular Member Hisato Matsumiya
Kyoto University Fellow Member Tomomi Yagi
Kyoto University Student Member Minh Thu Dao
Kyoto University Regular Member Kyohei Noguchi

1. INTRODUCTION

Stay cables experience different types of aerodynamic instabilities and are subjected to aerodynamic static forces. Extensive research has been conducted for more effective wind-resistant design and better stability by mitigating different types of vibrations and reducing aerodynamic forces. Different surface modifications are applied to control the flow around the body. One of these methods is the placement of surface spiral protuberances on the cable which significantly reduced the drag force and mitigated rain-wind induced vibrations and dry state galloping (Yagi et al., 2011). However, the mechanism behind the drag reduction, which appears in comparatively low Reynolds number (*Re*), is still under investigation and this study is an attempt to understand the mechanism.

2. OBJECTIVE AND METHODOLOGY

The aim of this study is to understand the effect of the spiral protuberances on the flow separation and the vortex shedding formed in the wake of the circular cylinder. By investigating the local influences of the protuberances on the flow separation and extending it to the whole scale of the cable, the effect of the spiral configuration of the protuberance on the drag crisis phenomenon could be examined. Pressure measurements were conducted in a wind tunnel on a smooth circular cylinder, and a cylinder with 12 spiral protuberances (Figure 1). The diameter of the cylinder was D= 0.07 m, and its length was 0.90 m. The protuberances were made of rubber, were 3.36 mm in width and 2.00 mm in thickness, and were placed on the surface with a winding angle $\gamma = 27°$ (Figure 2). Measurements were collected at different cross-sections in the spanwise direction (z) of the cable in a local scale (distance between two protuberances = 1 pitch = 22.9 mm) and the whole scale of the cable. The examined Reynolds numbers corresponded to the critical range ($1.3 \times 10^4 < Re < 2.5 \times 10^4$) and supercritical range ($Re > 2.5 \times 10^4$) for the spiral case, and the subcritical regime for the smooth cylinder. For the spiral case, the drag crisis and the suppression of the vortex shedding intensity (represented by the fluctuating lift force coefficient $C_L{}'$) were observed in the critical Reynolds regime (Figure 3).

Figure 1: The cylinder with 12 spiral protuberances.

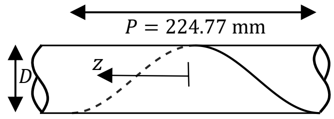

$\gamma = \tan^{-1}2D/P = 27°$

Figure 2: Illustration of the winding angle γ of the protuberances. P is the spanwise length of when the protuberances proceed one time around the cable.

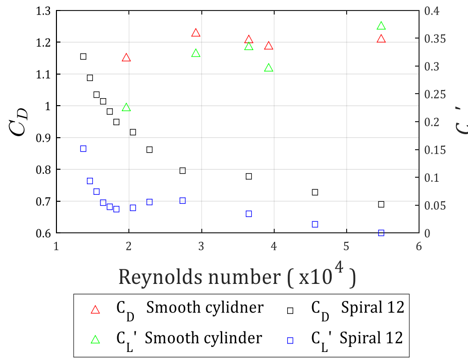

Figure 3: The drag coefficient (C_D) and the fluctuating lift force coefficient (C_L') for the smooth cylinder and the spiral case.

3. SPANWISE FLOW SEPARATION PATTERN

The spanwise flow separation pattern was examined for different Reynolds numbers in the spiral case in the upper and the lower halves of the cylinder. The flow separation location is determined to be at the location where the gradient of the mean pressure coefficient became zero while moving further downstream. Yagi et al. (2011) stated that there was a three-dimensionality observed as the flow separation point varied along the whole cable axis at every 1-pitch step. As for the flow separation pattern on the local scale, graphs in Figure 4 (a) and (b) are plotted for the upper half and the lower half respectively. From the graphs, two effects controlled the flow separation on the local scale. The first was the protuberance effect. At a fixed Reynolds number, the protuberances resulted in a direct separation at the tip of the protuberances. The flow separation will tend to follow the same path as the protuberance while moving in the z-direction. The second effect was the Reynolds number effect. When increased, it caused the flow separation to happen at a larger angle from the stagnation point. In the upper half, as a result of the winding direction of the protuberances, the angle of the protuberances increased while moving in the z-direction. With the increase of the Reynolds number, while moving in the

Keywords: drag crisis, vortex shedding, circular cylinder, spiral protuberances, state switching, correlation coefficient
Contact address: Kyoto University, Department of Civil and Earth Resources Eng., Kyoto, 615-8540, TEL 075-383-3167

z-direction, the flow was able to separate at a larger angle more easily with the support of the protuberance effect. On the other hand, in the lower half, the angle of the protuberances decreased while moving in the *z*-direction. With the increase of the Reynolds number, it was harder for the flow to keep separating at larger angle because the protuberance effect directed the flow to separate at a smaller angle from stagnation. This caused the flow separation pattern to transition back and forth more often than in the upper half. This asymmetry between the lower and the upper halves appeared more in the critical Reynolds number range ($U = 3$ m/s, and 4 m/s) indicating a three-dimensionality in the local scale. The spatial transitions in the flow separation location that happened on the local scale in the spanwise direction resulted in the state switching phenomenon. The phenomenon had a dominant low normalized frequency ($fD/U < 0.05$, where f is the frequency [Hz]) and appeared as non-symmetric states in form of jumps in the time series of the surface pressure (Figure 5). In the supercritical range ($U = 8$ m/s), the Reynolds number was high enough and the flow was able to counter the protuberance effect resulting in a more continuous separation pattern within 0.5 pitch.

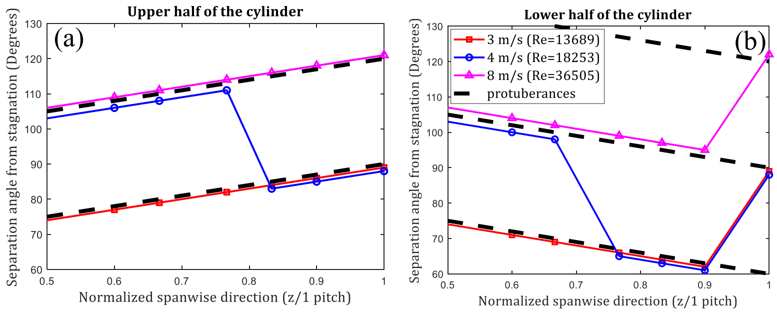

Figure 4: Flow separation pattern within the local scale in (a) the upper half and (b) the lower half of the cylinder.

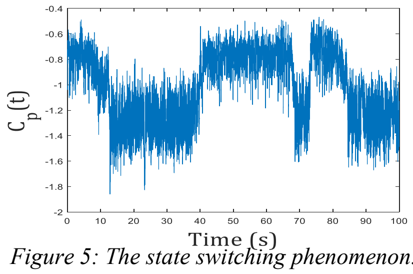

Figure 5: The state switching phenomenon. This pressure signal observed at pressure tap at 280° from stagnation at U=3.8 m/s (Re=17340)

4. SPANWISE VORTEX SHEDDING PATTERN

The spanwise correlation of the vortex shedding pattern is examined by looking at the spanwise correlation coefficient of the pressure signals on the whole scale of the cable. The Pearson correlation coefficient at a certain measurement point in the spanwise direction was calculated in reference to the first point (Figure 6). The correlation coefficient in the spiral case is much lower than the smooth cylinder case indicating a broken spanwise synchronization of the vortex shedding. This goes in accordance with the results recorded by Kleissl and Georgakis (2012). However, the correlation coefficient increased when using a bandpass filter from normalized frequency 0.15 to 0.25 on the pressure signal, that is, only the vortex shedding (Strouhal number $St \approx 0.2$) was considered and the state switching phenomenon was not considered. Therefore, the state switching seems to be the reason behind the broken spanwise coherence of the vortex shedding pattern. Consequently, the vortex shedding intensity was suppressed and the drag crisis happened in the critical Reynolds number regime. In the supercritical Reynolds number regime, the drag recovery was not observed and the drag coefficient remained constant around 0.7. This was because turbulent vortex shedding was not observed in the supercritical Reynolds regime.

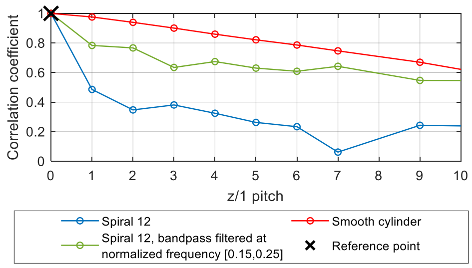

Figure 6: The spanwise correlation coefficient calculated at 90° from stagnation at U=5 m/s.

5. CONCLUSION

1. The spiral configuration of the protuberances resulted in a three-dimensionality of the flow that extended from the local to the global scale. The three-dimensionality resulted in the state switching phenomenon that appeared in the critical Reynolds number regime.

2. The state switching seems to have brought down the spanwise correlation coefficient and the synchronization of the vortex shedding pattern between different cross sections in the global scale. This caused the vortex shedding intensity to be significantly suppressed and the drag crisis occurred in the critical Reynolds number regime.

REFERENCES

Kleissl K., Georgakis C. (2012). “Comparison of the aerodynamics of bridge cables with helical fillets and a pattern-indented surface”. Journal of Wind Engineering and Industrial Aerodynamics 104-106, Pp (166-175).

Yagi T., Okamoto K., Sakaki I., Koroyasu H., Liang Z., Narita S., Shirato H. (2011). “Modification of surface configurations of stay cables for drag force reduction and aerodynamic stabilization”. The 21st National Symposium on Wind Engineering.